1-1-1988

A Mathematical Model for the Electrodeposition of Alloys on a Rotating Disk Electrode

Shiuan Chen
Texas A & M University - College Station

Ken-Ming Yin
Texas A & M University - College Station

Ralph E. White
University of South Carolina - Columbia, white@cec.sc.edu

Publication Info

Journal of the Electrochemical Society, 1988, pages 2193-2200.

http://www.electrochem.org
DOI: 10.1149/1.2096238
http://dx.doi.org/10.1149/1.2096238

surfaces being transformed by contact with reagent. Zero-time contact angles are 50°-80° and drop to values below 30° in a few minutes. As wetting changes with time, we have to acknowledge that it will also change from point to point, at the electrode surface, because the extent of reaction and the degree of product accumulation at different points cannot be the same. Two contiguous regions may thus present differences in θ amounting to some tens of degrees, depending on their actual compositions.

Now, we should consider the concentration effects. Added surfactants or acid will adsorb at the existing solid surfaces: both bare metal and reaction products (iron oxide, iron sulfate). Extent of adsorption will depend on the nature of the surface and on absorbate concentration. In the case of surfactants, we should expect that high concentrations will lead to saturation or to hemimicelle formation, so that the various solid surfaces will have their surface tension differences covered up. This means that low detergent concentration may both increase or decrease interfacial tension gradients; high concentrations should decrease them. Liquid circulation around the electrode and corrosion rates should vary accordingly, as indeed we found in this work.

Regarding sulfuric acid concentration changes, there is a major difference: we should not expect cover up of solids, due to the fact that at least bare patches of metal should not be saturated with the reactive acid. Indeed, the corrosion rates *vs.* acid concentration curve has a maximum, but the corrosion rate is still high at the higher acid concentration.

A major difficulty which is already seen in the process of creating a detailed model to evaluate convective liquid displacement around the electrode is that we need values for $\Delta\gamma$ and thus for interfacial tensions; since we are looking at reaction transients, the relevant γ's are dynamic, not equilibrium ones.

Manuscript submitted April 6, 1987; revised manuscript received Feb. 26, 1988.

Instituto de Fisica and Instituto de Química, UNICAMP, assisted in meeting the publication costs of this article.

REFERENCES

1. F. M. Donahue, A. Akiyama, and K. Nobe, *This Journal*, **114,** 1006 (1967).
2. W. E. O'Grady, *ibid.*, **127,** 555 (1980).
3. K. Kuroda, B. D. Cahan, G. Nazri, E. Yeager, and T. E. Mitchell, *ibid.*, **129,** 2163 (1982).
4. W. J. Lorenz and F. Mansfeld, "Interface and Interphase Inhibition," Proceedings of International Workshop on Corrosion Inhibition, NACE, Dallas, TX, May 1983.
5. H. Kaesche and N. Hackerman, *This Journal*, **105,** 191 (1958).
6. O. Teschke, F. Galembeck, and M. A. Tenan, *ibid.*, **132,** 1284 (1985).
7. O. Teschke and F. Galembeck, *ibid.*, **131,** 1095 (1984).
8. A. W. Adamson, "Physical Chemistry of Surfaces," 4th ed., p. 110, John Wiley & Sons, Inc., New York (1982).

A Mathematical Model for the Electrodeposition of Alloys on a Rotating Disk Electrode

Shiuan Chen, Ken-Ming Yin,* and Ralph E. White**

Department of Chemical Engineering, Texas A&M University, College Station, Texas 77843

ABSTRACT

A general multiple electrode reaction model for electrodeposition of alloys on a rotating disk electrode is presented. Included in the model are mass transport equations with the effect of ionic migration, Butler-Volmer kinetic rate expressions, and the mole fractions of the individual components in the solid state. The model shows that the effect of ionic migration is important and that plating variables such as applied potential, pH, and bulk concentration can be included. Two examples (Ni-P and Ru-Ni-P) are used to illustrate the predictions of the model.

One of the less expensive and most popular techniques for preparing alloys is electrodeposition (1). Electrodeposition from aqueous electrolyte solutions has considerable advantages over the other means of production of alloys because the technique is relatively easy, technically simple, fast and productive, and for certain systems is the only method of preparation. Therefore, it is desirable to determine the operating conditions under which a certain alloy can be made. A mathematical model which includes the effect of ionic migration is presented here as an aid to do this.

Two purely theoretical cases are presented here as examples of how the model may be used. These are the electrodeposition of Ni-P and Ru-Ni-P. Nickel-phosphorus alloys have received considerable attention (2-10) due to their ferromagnetic and metallic properties. The structure of Ni-P was investigated by Tyan and Toth (7); they found that alloys with a phosphorus composition greater than Ni-$P_{0.144}$ appeared to be amorphous. The dependence of the amorphous structure on the contents of the plating bath is supported by the work of Okamoto and Fukushima (5) and by Vafaei-Makhsoos (6). Analysis of the data from these experimental studies suggests that a theoretical model may be helpful in determining the operating conditions of a cell to produce such an alloy. The electrochemical reactions that are used here for electrodeposition of Ni-P are shown in Table I. The chemical species added are assumed to be $NiSO_4$, H_3PO_2. The evolution of hydrogen is included and is written as shown because it is the reaction that occurs as the potential of the working electrode is made more and more negative. To demonstrate the versatility of the model, the electrodeposition of a tertiary system Ru-Ni-P is also studied theoretically. The plating bath for this alloy contains $NiSO_4$, $NiCl_2$, H_3PO_2, and $RuCl_3$. Table II lists the electrochemical reactions that are assumed to participate in the deposition of Ru-Ni-P. The electrochemical system used to model these processes is that for a rotating disk electrode (RDE), which is used because of the simplicity of the system and its well-understood hydrodynamics (11, 12).

Table I. Reactions for Ni-P deposition

No.	Electrochemical reaction	Standard electrode potential, (V)[a]
1.	$Ni^{2+} + 2e^- \rightarrow Ni$	−0.23
2.	$H_3PO_2 + H^+ + e^- \rightarrow P + 2H_2O$	−0.51
3.	$2H^+ + 2e^- \rightarrow H_2$	0.00

[a]Taken from Ref. (30).

*Electrochemical Society Student Member.
**Electrochemical Society Active Member.

Table II. Reactions for Ru-Ni-P deposition

No.	Electrochemical reaction	Standard electrode potential, (V)[a]
1.	$RuCl_5^{2-} + 3e^- \rightarrow Ru + 5Cl^-$	+0.40
2.	$Ni^{2+} + 2e^- \rightarrow Ni$	−0.23
3.	$H_3PO_2 + H^+ + e^- \rightarrow P + 2H_2O$	−0.51
4.	$2H^+ + 2e^- \rightarrow H_2$	0.

[a]Taken from Ref. (30).

Most of the available models for electrodeposition are restricted to pure metals, and the convective and ionic migration effects are ignored for simplicity (13-15). The electrodeposition of alloys, compared with the electrodeposition of pure metals, is a much more complicated process. Some models (16-23) have been presented for binary alloy deposition. Their use is restricted, however, because these models (16-18) do not include the relative activities of the deposited species in the kinetic rate equation used. Also, none of these models includes the effect of ionic migration.

The relative activity of the deposited species was included in models developed by Engelken and Van Doren (20, 21), and Verbrugge and Tobias (22, 23). Engelken and Van Doren developed a steady-state model including only the diffusive transport mechanism for the electrodeposition of II-VI and III-IV compounds. Verbrugge and Tobias took into account the nonideal thermodynamic behavior in the solid state and modeled pulsed current electrodeposition processes for CdTe. Unfortunately, these models (20-23) do not include the effect of ionic migration.

The model presented here is an extension of previous models developed by White and coworkers (19, 24) which includes the effect of ionic migration. The effect of ionic migration is included in the model because of its fundamental importance in treating mass transfer in electrochemical systems. Its significance was reviewed by Vetter (25) and discussed by Newman [(26), p. 353]. Furthermore, Ateya and Pickering (27) investigated the effect of ionic migration under conditions of anodic dissolution. They found that if the initial concentration of the discharging ion is much less than that of the supporting electrolyte, the effect of ionic migration may be ignored, but if the metal ion/supporting ion concentration ratio varies considerably, as it may with distance from the electrode surface, then ionic migration may be significant.

In this model no interactions of deposited species are included (*i.e.*, activity coefficients for all solid components are one). This model could be used to handle a nonideal case if a suitable description for solid species interaction is available.

Model Development

The objective of the present investigation was to develop a detailed mathematical model which could be used to predict the concentration profiles of ionic species within a diffusion layer on an electrode, the current-potential characteristics, and the alloy compositions as a function of the bulk solution concentrations and the applied potential. The effect of ionic migration and the dependence of the current density on solid-state component relative activities are included.

The assumptions are as follows:

1. Dilute solution theory applies [(26), p. 217]. This states that there are negligible interactions between the solute species.
2. The Nernst-Einstein equation, $D_i = u_i RT$, which is implicit in the infinite dilute solution theory, applies.
3. The current density distribution is uniform on the surface of the electrode. Marathe and Newman (28) have shown that for small disks with an excess of supporting electrolyte, a uniform current density distribution can be assumed unless the exchange current density is large. In any case, the results apply at the center of the disk with this assumption.
4. The current density takes the form of the Butler-Volmer equation, which expresses the dependence of the current on the composition of the electrolytic solution adjacent to the electrode surface and on the relative activity of the solid-state species, and the exponential dependence of the current on the overpotential.
5. The physical, transport, and kinetic parameters are constant throughout the solution.
6. The solution is isothermal.
7. No homogeneous chemical reactions occur in the electrolyte.
8. The alloy exhibits ideal solid solution behavior.

The transport equation that applies in the diffusion layer is based on the flux equation of the ionic species in solution. Mass transport in solution is due to migration in an electric field, diffusion in a concentration gradient, and convection in a flow field. Therefore, the flux expression for each species i can be written as

$$\mathbf{N}_i = -z_i u_i \mathbf{F} c_i \nabla\Phi - D_i \nabla c_i + \mathbf{v} c_i \qquad [1]$$

where the ionic mobility, u_i, is assumed to be related to the diffusion coefficient D_i by the Nernst-Einstein equation

$$u_i = \frac{D_i}{RT} \qquad [2]$$

The material balance equation for each ionic species at every point within the diffusion layer is as follows

$$\frac{\partial c_i}{\partial t} = -\nabla \cdot \mathbf{N}_i + R_i \qquad [3]$$

where R_i is the production rate of species i due to homogeneous chemical reactions. For the rotating disk, the normal component of the velocity depends only on the direction normal to the electrode surface, y. Therefore, for steady-state analyses ($\partial c_i/\partial t = 0$) with no homogeneous reactions ($R_i = 0$), Eq. [3] combined with Eq. [1] becomes

$$D_i \frac{d^2 c_i}{dy^2} - v_y \frac{dc_i}{dy} + z_i u_i \mathbf{F}\left(c_i \frac{d^2\Phi}{dy^2} + \frac{dc_i}{dy}\frac{d\Phi}{dy}\right) = 0 \qquad [4]$$

where v_y in the diffusion layer is approximated by [(26), p. 282]

$$v_y = -a\Omega\left(\frac{\Omega}{\nu}\right)^{1/2} y^2 \qquad [5]$$

For convenience, a dimensionless distance, ξ, is defined by

$$\xi = \frac{y}{\delta} \qquad [6]$$

where δ is the diffusion layer thickness expressed as (19)

$$\delta = \left(\frac{3D_R}{a\nu}\right)^{1/3}\left(\frac{\nu}{\Omega}\right)^{1/2} \qquad [7]$$

in which D_R, ν, a, and Ω represent the diffusion coefficient of the diffusion-controlling species, kinematic viscosity, constant of the diffusion layer thickness, and the disk rotation speed, respectively. Expressed in terms of this dimensionless variable, Eq. [4] becomes

$$\frac{D_i}{D_R}\frac{d^2 c_i}{d\xi^2} + 3\xi^2 \frac{dc_i}{d\xi} + \frac{z_i D_i \mathbf{F}}{D_R RT}\left(c_i \frac{d^2\Phi}{d\xi^2} + \frac{dc_i}{d\xi}\frac{d\Phi}{d\xi}\right) = 0 \qquad [8]$$

With n ionic species present in the solution, there are a total of $n + 1$ unknowns, which are the n concentrations of the species and the solution potential, Φ. To solve for these $n + 1$ unknowns, $n + 1$ governing equations are needed. These are given by the n material balance equations (Eq. [8]) plus the equation of electroneutrality

$$\sum_{i=1}^{n} z_i c_i = 0 \quad [9]$$

for every point in the electrolyte, $0 \le y < y_{RE}$, where y_{RE} represents the location of the reference electrode.

Boundary conditions at $y = y_{RE}$ are chosen where the concentration of each species i near the reference electrode is equal to its bulk concentrations

$$c_i(y_{RE}) = c_{i,bulk} \quad [10]$$

where the values for $c_{i,bulk}$ satisfy Eq. [9]. The boundary condition for the solution potential is

$$\Phi(y_{RE}) = \Phi_{RE} \quad [11]$$

Experimentally, $V - \Phi(y_{RE})$ is the potential that is applied, and only this difference makes physical sense. Consequently, it is acceptable to set arbitrarily $V = 0$ and use Φ_{RE} as the value of the applied potential.

The boundary conditions at the electrode surface (at $y = 0$) are obtained from a component material balance equation at the electrode. The condition is that the normal component of the flux of species i evaluated at the surface is equal to the sum of its reaction rates at the electrode

$$\mathbf{N}_i|_{y=0} = -\sum_{j=1}^{NR} \frac{s_{ij} i_j}{n_j \mathbf{F}} \quad [12]$$

where NR is the number of reactions occurring at the electrode surface, s_{ij} is the stoichiometric coefficient of species i of reaction j, and n_j is the number of electrons transferred in reaction j when the reaction is written in the form

$$\sum_i s_{ij} M_i^{z_i} \rightarrow n_j e^- \quad [13]$$

At the electrode surface, the normal component of the velocity is zero. Consequently, Eq. [1] reduces to

$$\mathbf{N}_i|_{y=0} = -\frac{z_i D_i \mathbf{F} c_i}{RT}\frac{d\Phi}{dy} - D_i \frac{dc_i}{dy} \quad [14]$$

when expressed in dimensionless form

$$\mathbf{N}_i|_{\xi=0} = -\frac{1}{\delta}\left(D_i \frac{dc_i}{d\xi} + \frac{z_i D_i \mathbf{F} c_i}{RT}\frac{d\Phi}{d\xi}\right) \quad [15]$$

Combination of Eq. [12] and [15] gives the final boundary condition of the system at the electrode surface

$$-\frac{1}{\delta}\left(D_i \frac{dc_i}{d\xi} + \frac{z_i D_i \mathbf{F} c_i}{RT}\frac{d\Phi}{d\xi}\right) = -\sum_{j=1}^{NR} \frac{s_{ij} i_j}{n_j \mathbf{F}} \quad [16]$$

Equation [16] provides n equations for n number of species. The last boundary condition at the surface is the electroneutrality requirement, Eq. [9].

The current density due to reaction j as in Eq. [16] is assumed to take the form of the Butler-Volmer equation [(26), p. 169]

$$i_j = i_{oj}\left[\exp\left(\frac{\alpha_{aj}\mathbf{F}}{RT}\eta_j\right) - \exp\left(\frac{-\alpha_{cj}\mathbf{F}}{RT}\eta_j\right)\right] \quad [17]$$

This can be regarded as the result of independent cathodic and anodic reactions, each with an exponential dependence on the overpotential η_j, where

$$\eta_j = V - \Phi_o - U_{j,o} \quad [18]$$

The quantity $V - \Phi_o$ represents the potential difference between the potential of the electrode (V), and the potential in the solution adjacent to the electrode (Φ_o). The theoretical open-circuit potential, $U_{j,o}$, evaluated at the surface concentrations of all the species, $c_{i,o}$, and solid phase relative activities, $a_{k,o}$, is expressed by (19)

$$U_{j,o} = U_j^\theta - \frac{RT}{n_j \mathbf{F}}\left[\sum_i s_{ij} \ln\left(\frac{c_{i,o}}{\rho_o}\right) + \sum_k s_{kj} \ln a_{k,o}\right] - U^\theta_{RE} + \frac{RT}{n_{RE}\mathbf{F}}\sum_i s_{i,RE} \ln\left(\frac{c_{i,RE}}{\rho_o}\right) \quad [19]$$

The exchange current density i_{oj} depends on the concentration in the solution at the electrode-electrolyte interface and the relative activity of the metallic species in the deposited alloy. That is, i_{oj} is assumed to have the following form

$$i_{oj} = i_{oj,ref}\prod_i \left(\frac{c_{i,o}}{c_{i,ref}}\right)^{\gamma_{ij}} \prod_k \left(\frac{a_{k,o}}{a_{k,ref}}\right)^{\gamma_{kj}} \quad [20]$$

where $a_{k,ref}$ is a reference relative activity of metallic species k, and $c_{i,ref}$ is a reference concentration of species i. Note $i_{oj,ref}$ can be expressed by

$$i_{oj,ref} = i_{oj,data}\prod_i \left(\frac{c_{i,ref}}{c_{i,data}}\right)^{\gamma_{ij}} \prod_k \left(\frac{a_{k,ref}}{a_{k,data}}\right)^{\gamma_{kj}} \quad [21]$$

$i_{oj,ref}$ can be calculated if $i_{oj,data}$, $c_{i,data}$ $a_{k,data}$ are available in the literature; otherwise, experiments need to be devised to determine $i_{oj,ref}$ using parameter estimation techniques.

In both Eq. [19] and [20], the subscript i ranges over the ionic species and k over the metallic species. The exponents for both the ionic and metallic species are given by (24)

$$\gamma_{ij} = p_{ij} - \frac{\alpha_{aj} s_{ij}}{n_j} \quad [22]$$

for an anodic reactant, and

$$\gamma_{ij} = q_{ij} + \frac{\alpha_{cj} s_{ij}}{n_j} \quad [23]$$

for a cathodic reactant. Similar expression is used for γ_{kj}.

The open-circuit potential $U_{j,o}$ can be written in terms of the reference concentrations by adding and subtracting the following term to Eq. [19]

$$\frac{RT}{n_j \mathbf{F}}\sum_i s_{ij} \ln\left(\frac{c_{i,ref}}{\rho_o}\right) + \frac{RT}{n_j \mathbf{F}}\sum_k s_{kj} \ln a_{k,ref} \quad [24]$$

The result is

$$U_{j,o} = U_{j,ref} - \frac{RT}{n_j \mathbf{F}}\left[\sum_i s_{ij} \ln\left(\frac{c_{i,o}}{c_{i,ref}}\right) + \sum_k s_{kj} \ln\left(\frac{a_{k,o}}{a_{k,ref}}\right)\right] \quad [25]$$

where

$$U_{j,ref} = U_j^\theta - \frac{RT}{n_j \mathbf{F}}\left[\sum_i s_{ij} \ln\left(\frac{c_{i,ref}}{\rho_o}\right) + \sum_k s_{kj} \ln a_{k,ref}\right] - \left[U^\theta_{RE} - \frac{RT}{n_{RE}\mathbf{F}}\sum_i s_{ij} \ln\left(\frac{c_{i,RE}}{\rho_o}\right)\right] \quad [26]$$

Note the solid phase compositions are involved in both the expression of i_{oj} and $U_{j,o}$. Combining Eq. [17], [18], [20], [22], [23],and [25] yields

$$i_j = i_{oj,ref}\left\{\prod_i \left(\frac{c_{i,o}}{c_{i,ref}}\right)^{p_{ij}} \prod_k \left(\frac{a_{k,o}}{a_{k,ref}}\right)^{p_{kj}} \exp\left[\frac{\alpha_{aj}\mathbf{F}}{RT}(V - \Phi_o - U_{j,ref})\right] - \prod_i \left(\frac{c_{i,o}}{c_{i,ref}}\right)^{q_{ij}} \prod_k \left(\frac{a_{k,o}}{a_{k,ref}}\right)^{q_{kj}} \exp\left[\frac{-\alpha_{cj}\mathbf{F}}{RT}(V - \Phi_o - U_{j,ref})\right]\right\} \quad [27]$$

In addition, the anodic and cathodic transfer coefficients are assumed to sum to the number of electrons transferred for reaction j (*i.e.*, $\alpha_{aj} + \alpha_{cj} = n_j$), and the reaction order constants are assumed to be simply related to s_{ij}

$$p_{ij} = s_{ij} \qquad q_{ij} = 0 \qquad \text{if } s_{ij} > 0$$

$$p_{ij} = 0 \qquad q_{ij} = -s_{ij} \qquad \text{if } s_{ij} < 0 \qquad [28]$$

The relative activities of the solid solution phase components $a_{k,o}$ shown in Eq. [27] are unknown variables. They are determined by first assuming that the solid solution is ideal so that the relative activity of solid species k can be approximated by the mole fraction in the solid phase

$$a_{k,o} \simeq x_{k,o} \qquad [29]$$

The next step is to assume that the mole fraction of solid species k is given by the ratio of the deposition rate of species k to the total rate of deposition of all of the solid solution species

$$x_{k,o} = \frac{r_k}{(r_1 + r_2 + \cdots + r_m)} \qquad [30]$$

where m is the total number of solid solution species, and the deposition rate of species k is given by

$$r_k = \sum_{j=1}^{NR} \frac{s_{kj} i_j}{n_j \mathbf{F}} \qquad [31]$$

where the current density in the rate expression is given by Eq. [27]. The substitution of Eq. [31] into Eq. [30] yields

$$x_{k,o} = \frac{\sum_{j=1}^{NR} \frac{s_{kj} i_j}{n_j \mathbf{F}}}{\sum_{l=1}^{m} \sum_{j=1}^{NR} \frac{s_{lj} i_j}{n_j \mathbf{F}}} \qquad [32]$$

The inclusion of the dependence on solid-state relative activities in the Butler-Volmer equation introduces the mole fractions ($x_{k,o}$) as new unknowns. With this addition of m new unknowns, which are the mole fractions for each solid species, m new equations are needed to complete the system of independent equations. Equation [32] provides m − 1 of these equations and the m^{th} equation is simply that the mole fractions have to sum to one

$$\sum_{k=1}^{m} x_{k,o} = 1 \qquad [33]$$

Finally, after setting the operating conditions and the kinetic, transport, and thermodynamic parameters, the total predicted current density (i_T) at a set potential difference ($V - \Phi_{RE}$) is obtained by summing the current densities for each reaction

$$i_T = \sum_{j=1}^{NR} i_j \qquad [34]$$

The boundary value problem posed above is solved by using BAND(J), a finite difference numerical technique developed by Newman [(26), p. 414]. The derivatives in the coupled, second-order differential equations are approximated with finite differences. Three point central differences accurate to the order of h^2, where h is the dimensionless step size used in the solution field, are used. The boundary conditions at y_{RE} where the reference electrode located are the fixed values of bulk species concentrations and the applied potential as discussed before. The flux boundary conditions at the electrode surface are approximated by backward differences. The mole fractions ($x_{k,o}$) of the components in the solid phase are treated by using a constant variable approach (29). Physically x_k has values only at $y = 0$ as described by Eq. [32]. But for computational convenience, we also employ the expression $dx_k/dy = 0$ for x_k in the region $0 < y < y_{RE}$. It should be noted that mole fractions are only calculated when more than one metal is deposited on the electrode surface. This is determined by the criterion that the second metal deposited is at least 0.03% of the deposited alloy.

Table III. Compositions of Ni-P alloy plating baths for pH analysis

Constituent	Concentration (M) I	II	III
Ni^{2+}	0.38	0.38	0.38
H_3PO_2	0.38	0.38	0.38
H^+	1.0×10^{-1}	1.0×10^{-3}	1.0×10^{-5}
SO_4^{2-}	0.580	0.5305	0.530005
Na^+	0.300	0.300	0.300
OH^-	1.0×10^{-13}	1.0×10^{-11}	1.0×10^{-9}
$a_{Ni,ref}$	0.50	0.50	0.50
$a_{P,ref}$	0.50	0.50	0.50

Results and Discussion

Nickel-phosphorus alloy.—The first theoretical case study consisted of determining the effect of the pH of the plating solution on the current density-potential profile and the composition of the deposit. Results are presented for the three plating solutions shown in Table III, where the pH is varied from 1 in bath I, to 3 in bath II, and then to 5 in bath III. The operating conditions and fixed parameters are given in Table IV. The nickel-to-phosphorus ratio in the bulk solution is 1:1 in all three plating baths. The predictions were terminated at $E_{appl} = -1.1$V because beyond this potential the hydrogen evolution reaction dominates the system.

As shown in Fig. 1, the solid line represents the results obtained from the plating solution pH = 1. The dotted and dashed curves, which completely overlap each other, represent the plating solutions of pH = 3 and 5, respectively. Also, the associated plot of the mole fraction of nickel and phosphorus *vs.* potential (Fig. 2) shows that practically no phosphorus is deposited from the plating solutions when the pH is greater than 3. Thus, it should be expected that a solution with a large pH would be poor for depositing phosphorus. It is interesting that the limiting current for nickel deposition is higher at the higher pH values in Fig. 1. This is due to the fact that at higher pH values more nickel ions are present at the electrode surface which gives rise to a large limiting current density value.

Also, it is important to note that the effect of ionic migration is significant in determining the predicted current-potential curves in Fig. 1. This is illustrated in Fig. 3-4. The solid line in Fig. 3 is the same as that in Fig. 1 for pH = 1; the dotted line in Fig. 3 was generated by the following procedure. First, for a given E_{appl} the corresponding solution potential profile was determined (*i.e.*, with the effect of migration included). Next, set Φ_o from that potential profile equal to a constant over the region $0 < y < y_{RE}$. Now, resolve the governing equations by taking out the electroneutrality condition and setting the mobility (u_i) for

Table IV. Operating conditions and parameter values for Ni-P alloy deposition

Parameter	Value
T	298.15 K
Ω	209.44 rad/s
ρ	1×10^{-3} kg/cm^3
ν	0.0123 cm^2/s
y_{RE}	0.02 cm
$D_{Ni^{2+}}$	0.71×10^{-5} cm^2/s[a]
$D_{H_3PO_3}$	1.54×10^{-5} cm^2/s[b]
D_{H^+}	9.312×10^{-5} cm^2/s[a]
$D_{SO_4^{2-}}$	1.065×10^{-5} cm^2/s[a]
D_{Na^+}	1.334×10^{-5} cm^2/s[a]
D_{OH^-}	5.260×10^{-5} cm^2/s[a]
$\alpha_{a,1}$	0.5[c]
$\alpha_{c,1}$	1.5
$\alpha_{a,2}$	0.5[d]
$\alpha_{c,2}$	0.5
$\alpha_{a,3}$	0.5[d]
$\alpha_{c,3}$	0.5
$i_{o1,ref}$	1.0×10^{-6} A/cm^2[d]
$i_{o2,ref}$	1.0×10^{-4} A/cm^2[d]
$i_{o3,ref}$	6.3×10^{-10} A/cm^2[d]

[a]Taken from Ref. (26).
[b]Calculated from Ref. (33).
[c]Taken from Ref. (32).
[d]Chosen to agree qualitatively with experimental data (31).

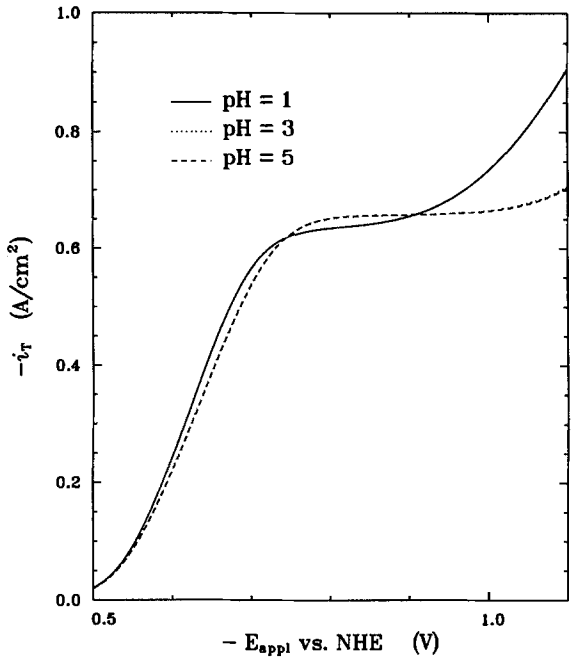

Fig. 1. Effect of the pH of the plating bath on the current density-potential relationship for the deposition of Ni-P.

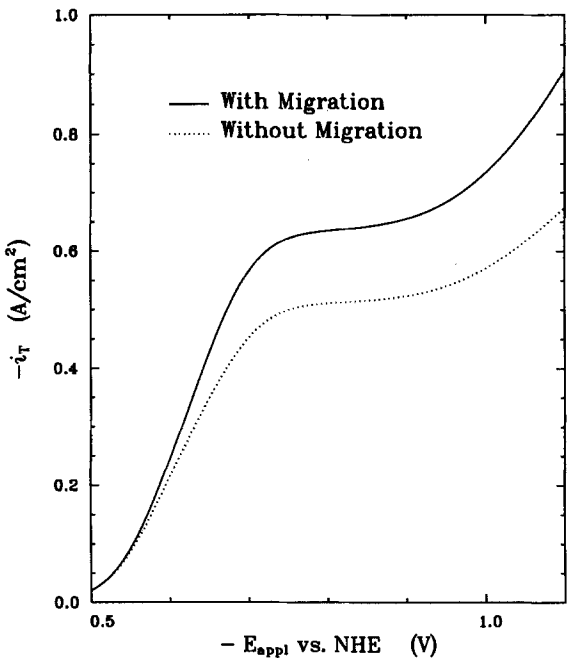

Fig. 3. Comparison of total current obtained with and without the effect of migration on Ni-P deposition.

each species equal to zero. Finally, calculate a new total current density and plot as a point on the dotted line in Fig. 3. As shown in Fig. 3, taking out the effect migration at low values of E_{appl} does not change the total current density because in this region the surface overpotential limits the process (kinetic control). As $-E_{appl}$ is made larger, transport resistance becomes important. Note that the limiting current density for nickel deposition for this case as calculated by the Levich equation (34) is -0.506 A/cm^2. Further illustration of the influence of including ionic migration can be seen from the concentration profiles in Fig. 4, where it can be seen that a significantly larger Ni^{+2} concentration gradient exists at the surface of the electrode when migration effects are included. Apparently, the reason for this is the indirect influence of the electroneutrality condition (*i.e.*, the potential) through the other species and not the small migration part of the flux of Ni^{2+}. The effect of migration on the alloy composition is minor except at large $-E_{appl}$, for example at $-E_{appl} = 1.0$, the phosphorus mole fraction is 20% when including the effect of migration, compared to 17% when not considering migration.

Next the effect of the relative metal content in the bulk solution is considered. Results are presented for three plating baths whose compositions are shown in Table V. The total metal content in the solution is kept constant at 0.76*M* and the amount of hypophosphorus acid is varied from 25 mole percent (m/o) in plating bath I, to 50 m/o in bath II and to 75 m/o in bath III. The pH is maintained at one for all three solutions, and the operating conditions and the kinetic and transport parameter values are same as those listed in Table IV. Figures 5 and 6 are the resulting total current density-potential and composition-potential plots.

As seen in Fig. 5, the decrease in the nickel concentration in the bulk causes the limiting current density of the nickel reduction reaction to decrease accordingly. The cor

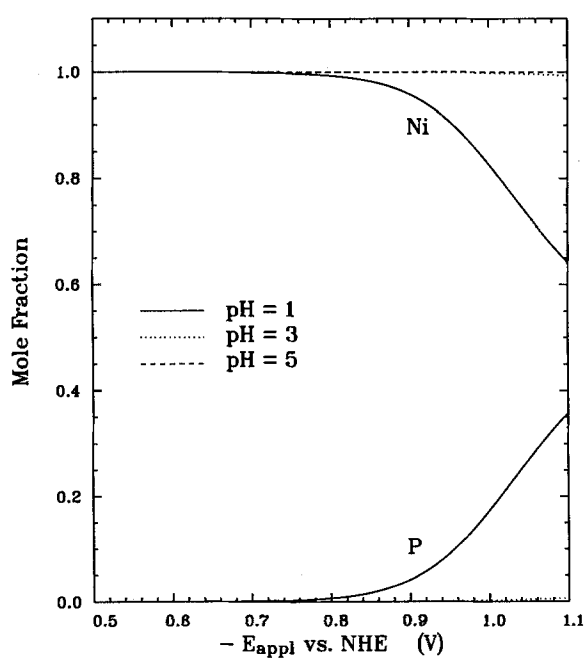

Fig. 2. Effect of the pH of the plating bath on the deposit composition for the deposition of Ni-P.

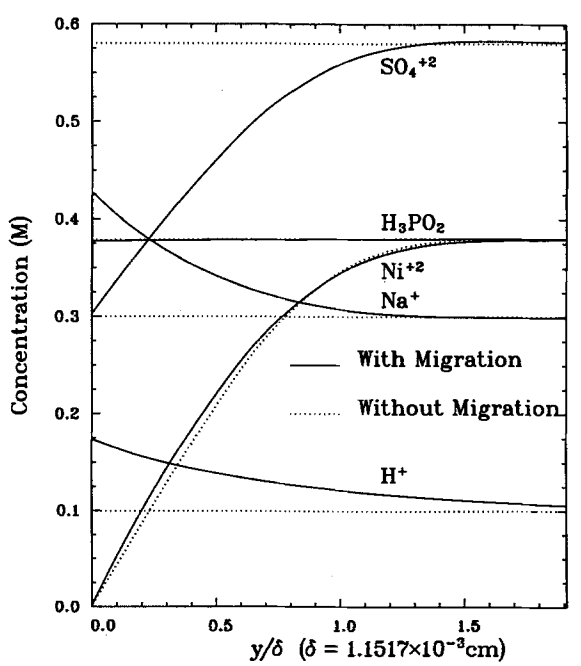

Fig. 4. Concentration profiles with and without the effect of migration at $-E_{appl} = 0.8$V.

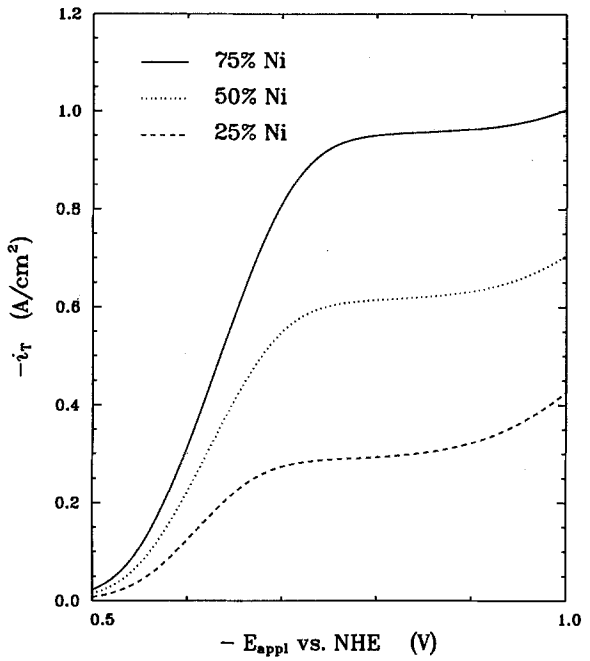

Fig. 5. Effect of the metal content in plating bath on the current density-potential relationship for the deposition of Ni-P.

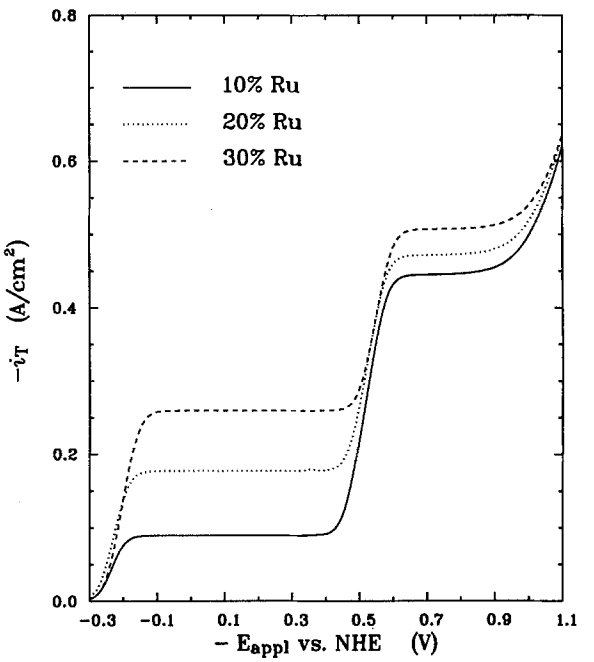

Fig. 7. Effect of the metal content in the plating bath on the current density-potential relationship for the deposition of Ru-Ni-P.

responding increase in hypophosphorus acid results in a sharper rise of current density at the potential region where phosphorus is deposited. The mole fraction *vs.* potential curves in Fig. 6 exhibits the behavior of preferential deposition of the more noble metal, nickel. This means that the nickel to phosphorus ratio in the deposit is much lower than the nickel to phosphorus ratio in the plating bath. Since the degree of crystallinity of Ni-P depends heavily on the amount of phosphorus present in the alloy, it is important to deposit the alloy at a large enough potential to ensure that the composition of phosphorus in the alloy is above the minimum required for the alloy to be amorphous. This threshold has been determined experimentally (7) to be 14.4%.

Ruthenium-nickel-phosphorus alloy.—Another alloy of interest to us is Ru-Ni-P. In solutions containing excess chloride ions, ruthenium tends to complex with chloride as follows

$$Ru^{2+} + 5Cl^- \rightleftharpoons RuCl_5^{2-}$$

The effect of the *p*H of the plating solution was also examined (31) for the electrodeposition of Ru-Ni-P. Results showed that the *p*H value has almost no effect on the amount of ruthenium deposited. The effect of *p*H on the nickel and phosphorus content in the alloy was very much the same as that for Ni-P alloy deposition. Practically no phosphorus can be deposited from solutions of *p*H > 3.

The dependence of the electrodeposition of Ru-Ni-P alloy on the relative metal content in the bulk solution was also examined and is presented here. The relevant fixed parameters and bulk concentrations are shown in Tables VI and VII. The total metal content in the solution is kept constant at 0.50*M* ($RuCl_5^{2-}$, Ni^{+2}, H_3PO_2). The nickel to phosphorus concentration ratio in solution is 1:1 for all three plating baths. The ruthenium contents for the three plating baths are 10%, 20%, and 30%, respectively. The *p*H is again maintained at one for all three solutions.

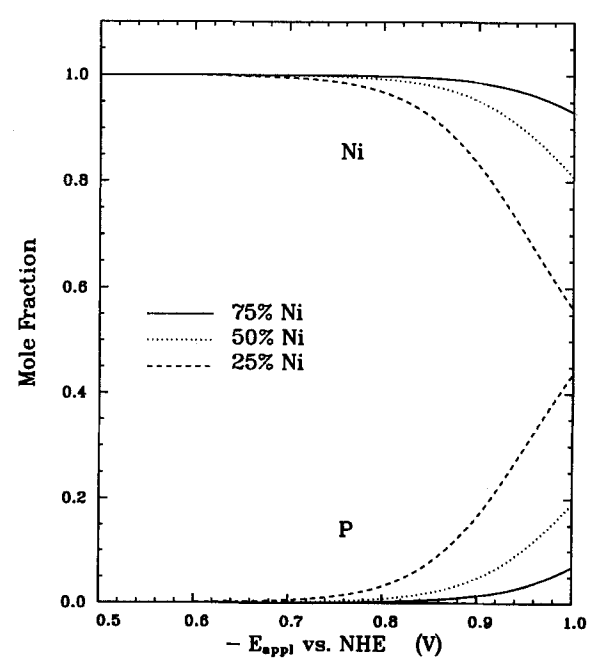

Fig. 6. Effect of the metal content in plating bath on the deposit composition for the deposition of Ni-P.

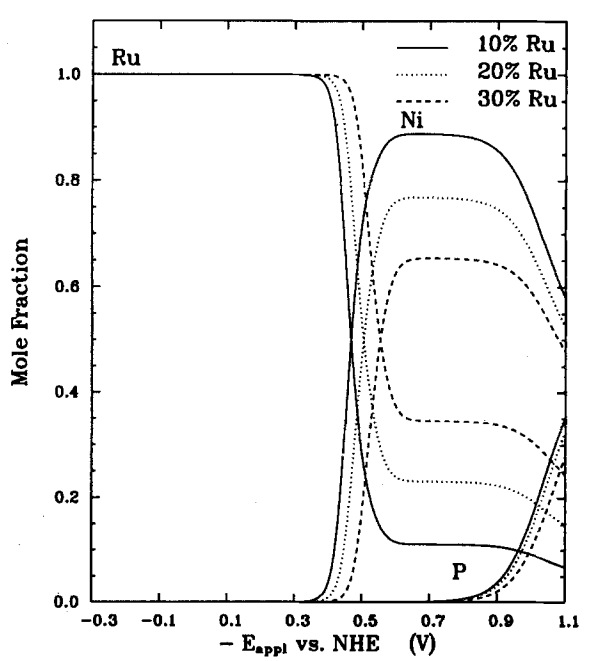

Fig. 8. Effect of the metal content in the plating bath on the deposit composition for the deposition of Ru-Ni-P.

Table V. Compositions of Ni-P alloy plating baths for metal content analysis

Constituent	Concentration (M) I	II	III
Ni^{2+}	0.57	0.38	0.19
H_3PO_2	0.19	0.38	0.57
H^+	0.10	0.10	0.10
SO_4^{2-}	0.87	0.68	0.49
Na^+	0.50	0.50	0.50
OH^-	1.0×10^{-13}	1.0×10^{-13}	1.0×10^{-13}
$a_{Ni,ref}$	0.50	0.50	0.50
$a_{P,ref}$	0.50	0.50	0.50

Figure 7 presents the current density potential relationships for the three baths, and Fig. 8 shows the predicted alloy composition. The current density of the ruthenium reaction increases as the ruthenium chloride in the plating bath increased, and that of the nickel reaction decreases as the nickel content is decreased. As shown in Fig. 8 the Ni species has higher tendency than Ru to deposit for $-E_{appl} > 0.6V$. It is very interesting to note here that both the ruthenium and nickel compositions varied accordingly as the bulk solution concentrations were varied. However, the amount of phosphorus predicted in the alloy is relatively independent of the variations in the bulk solution concentrations. This may indicate the amount of P deposit in the alloy depends more on the pH than on the bulk metal concentration. A more-in-depth consideration of the solution chemistry is probably necessary to analyze the importance of the pH of the bath in more depth.

Summary

A potentiostatic model for the electrodeposition of multicomponent alloys on a rotating disk electrode has been developed. The model can be used to predict a concentration profile for each species in the solution, current density-potential relationships, and alloy compositions in the deposit. The dependence of the current density on the solid-state component relative activities is included in the Butler-Volmer kinetic rate expression. The model is flexible and allows application to any multiple electrochemical reactions system, as demonstrated in this work. The accuracy of the results depends on the accuracy of the assumptions made about the bulk solution equilibrium, the hypothesized electrochemical reactions occurring on the electrode surface, and the accuracy of the kinetic and transport parameters used for the system. It is predicted that the effect of ionic migration is important for the systems considered here.

Table VI. Operating conditions and parameter values for Ru-Ni-P alloy deposition

Parameter	Value
T	298.15 K
Ω	209.44 rad/s
ρ	1×10^{-3} kg/cm^3
ν	0.0123 cm^2/s
y_{RE}	0.02 cm
$D_{RuCl_5^{2-}}$	0.86×10^{-5} cm^2/s[a]
D_{Cl^-}	2.032×10^{-5} cm^2/s[b]
$D_{Ni^{2+}}$	0.71×10^{-5} cm^2/s[b]
$D_{H_3PO_2}$	1.54×10^{-5} cm^2/s[a]
D_{H^+}	9.312×10^{-5} cm^2/s[b]
$D_{SO_4^{2-}}$	1.065×10^{-5} cm^2/s[b]
D_{Na^+}	1.334×10^{-5} cm^2/s[b]
D_{OH^-}	5.260×10^{-5} cm^2/s[b]
$\alpha_{a,1}$	1.5[c]
$\alpha_{c,1}$	1.5
$\alpha_{a,2}$	0.5[d]
$\alpha_{c,2}$	1.5
$\alpha_{a,3}$	0.5[c]
$\alpha_{c,3}$	0.5
$\alpha_{a,4}$	0.5[c]
$\alpha_{c,4}$	0.5
$i_{o1,ref}$	2.0×10^{-6} A/cm^2[c]
$i_{o2,ref}$	1.0×10^{-6} A/cm^2[c]
$i_{o3,ref}$	1.0×10^{-4} A/cm^2[c]
$i_{o4,ref}$	6.3×10^{-10} A/cm^2[c]

[a]Calculated from Ref. (33).
[b]Taken from Ref. (26).
[c]Chosen to agree qualitatively with experimental data (31).
[d]Taken from Ref. (32).

Table VII. Compositions of Ru-Ni-P alloy plating baths for metal content analysis

Constituent	Concentration (M) I	II	III
$RuCl_5^{2-}$	0.050	0.100	0.150
Ni^{2+}	0.225	0.200	0.175
H_3PO_2	0.225	0.200	0.175
H^+	0.100	0.100	0.100
Cl^-	0.200	0.200	0.200
SO_4^{2-}	0.225	0.200	0.175
Na^+	0.200	0.300	0.400
OH^-	1.0×10^{-13}	1.0×10^{-13}	1.0×10^{-13}
$a_{Ru,ref}$	0.333	0.333	0.333
$a_{Ni,ref}$	0.333	0.333	0.333
$a_{P,ref}$	0.333	0.333	0.333

Acknowledgment

The authors are grateful for the support of this project given by the Texas Advance Technology and Research Program, the Texas A&M University Board of Regents through the Available University Fund, and Sandia National Laboratories.

Manuscript submitted Aug. 11, 1986; revised manuscript received Feb. 29, 1988.

Texas A&M University assisted in meeting the publication costs of this article.

LIST OF SYMBOLS

a	0.51023
$a_{k,o}$	relative activity of metal k in the deposit
$a_{k,data}$	data relative activity of metal k
$a_{k,ref}$	reference relative activity of metal k in the deposit
c_i	concentration of species i, mol/cm^3
$c_{i,bulk}$	bulk solution concentration of species i, mol/cm^3
$c_{i,data}$	data concentration of species i, mol/cm^3
$c_{i,ref}$	reference concentration of species i, mol/cm^3
$c_{i,RE}$	concentration of species i for reference electrode reaction, mol/cm^3
D_i	diffusion coefficient of species i, cm^2/s
D_{RE}	diffusion coefficient of the diffusion controlling species, cm^2/s
E_{appl}	$V - \Phi_{RE}$, V
$\mathbf{F}$	Faraday's constant, 96,487 C/mol
h	mesh size
i_j	current density due to reaction j, A/cm^2
$i_{oj,o}$	exchange current density at surface concentrations for reaction j, A/cm^2
$i_{oj,data}$	exchange current density of concentrations reported in the literature ($c_{i,data}$), A/cm^2
$i_{oj,ref}$	exchange current density at reference concentrations for reaction j, A/cm^2
n_j	number of electrons transferred in reaction j
n_{RE}	number of electrons transferred in reference electrode reaction
$\mathbf{N}_i$	flux vector of species i, mol/cm^{2}s
NR	number of reactions
p_{ij}	anodic reaction order of species i in reaction j
q_{ij}	cathodic reaction order of species i in reaction j
r_k	rate of deposition of solid species k
R	universal gas constant, 8.3143 J/mol · K
s_{ij}	stoichiometric coefficient of species i in reaction j
T	absolute temperature, K
u_i	mobility of species i, mol · cm^2/Js
$U_{j,o}$	theoretical open-circuit potential for reaction j at the surface concentrations of species i, V
$U_{j,ref}$	theoretical open-circuit potential evaluated at reference concentrations, V
U^0_j	standard electrode potential for reaction j, V
U^0_{RE}	standard electrode potential for reference electrode reaction, V
$\mathbf{v}$	electrolyte velocity vector, cm/s
v_y	electrolyte velocity in the normal direction, cm/s
V	potential of the working electrode, V
$x_{k,o}$	mole fraction of metallic species k in the electrodeposit
y	normal coordinate, cm
y_{RE}	position of reference electrode, cm
z_i	charge number of species i

Greek Symbols

α_{aj}	anodic transfer coefficient for reaction j
α_{cj}	cathodic transfer coefficient for reaction j
γ_{ij}	exponent in composition dependence of exchange current density, i_{oj} on species i
δ	diffusion layer thickness, cm
η_j	overpotential for reaction j, V
ν	kinematic viscosity, cm^2/s
ξ	dimensionless distance ($\xi = y/\delta$)
ρ_o	pure solvent density, kg/cm^3
Φ	potential in solution within diffusion layer, V
Φ_o	solution potential adjacent to electrode surface, V
Φ_{RE}	potential in the bulk solution at y_{RE}, V
Ω	disk rotation velocity, rad/s

REFERENCES

1. R. B. Diegle, *Mater. Eng.*, **96,** 46 (1982).
2. "Symposium on Electroless Nickel Plating," American Society for Testing Materials, Pennsylvania (1959).
3. G. G. Gawrilov, "Chemical (Electroless) Nickel Plating," Portcullis Press, Redhill (1979).
4. T. Yamasaki, H. Izumi, and H. Sunada, *Scr. Metall.*, **15,** 177 (1981).
5. T. Okamoto and Y. Fukushima, *J. Non-Cryst. Solids,* **61,** 379 (1984).
6. E. Vafaei-Makhsoos, *J. Appl. Phys.*, **15,** 6366 (1980).
7. Y. S. Tyan and L. E. Toth, *J. Electron. Mater.*, **3,** 791 (1974).
8. B. G. Bagley and D. Turnbull, *J. Appl. Phys.*, **39,** 5681 (1968).
9. I. de Iorio, V. Tagliaferri, and L. Lanotte, *J. Met.*, November, 48 (1985).
10. A. Mayer, K. Staudhammer, and K. Johnson, *Plat. Surf. Finishing,* **72,** 76 (1985).
11. W. G. Cochran, *Proc. Cambridge Philos. Soc.*,**30,** 365 (1934).
12. M. H. Rogers and G. N. Lance, *J. Fluid Mech.*, **7,** 617 (1960).
13. K. I. Popov, B. J. Lazarević, and M. Kostić, *J. Appl. Electrochem.*, **3,** 161 (1973).
14. K. I. Popov, D. N. Keča, S. I. Vidojković, B. J. Lazarević, and V. B. Milojković, *ibid.*, **6,** 365 (1976).
15. Y. Ogata, K. Yamakawa, and S. Yoshizawa, *ibid.*, **12,** 439 (1982).
16. A. M. Pesco and H. Y. Cheh, Submitted to *This Journal.*
17. C. R. Beauchamp, Abstract 216, p. 332, The Electrochemical Society Extended Abstracts, Vol. 85-2, Las Vegas, Nevada, Oct. 13-18, 1985.
18. M. Menon and U. Landau, Abstract 217, p. 333, The Electrochemical Society Extended Abstracts, Vol. 85-2, Las Vegas, Nevada, Oct. 13-18, 1985.
19. R. E. White, J. A. Trainham, J. S. Newman, and T. W. Chapman, *This Journal,* **124,** 671 (1977).
20. R. D. Engelken and T. P. Van Doren, *ibid.*, **132,** 2904 (1985).
21. R. D. Engelken and T. P. Van Doren, *ibid.*, **132,** 2910 (1985).
22. M. W. Verbrugge and C. W. Tobias, *ibid.*, **132,** 1298 (1985).
23. M. W. Verbrugge and C. W. Tobias, *AIChE J.*, **33,** 628 (1987).
24. R. E. White, S. E. Lorimer, and R. Darby, *This Journal,* **130,** 1123 (1983).
25. K. Vetter, "Electrochemical Kinetics," p. 169, Academic Press, New York (1967).
26. J. S. Newman, "Electrochemical Systems," p. 230, Prentice Hall, Inc., Englewood Cliffs, NJ (1973).
27. B. G. Ateya and H. W. Pickering, *J. Appl. Electrochem.*, **11,** 453 (1981).
28. V. Marathe and J. S. Newman, *This Journal,* **116,** 1704 (1969).
29. T. V. Nguyen, M.S. Thesis, Texas A&M University, Texas (1985).
30. "Lange's Handbook of Chemistry," J. A. Dean, Editor, McGraw-Hill Book Co., New York (1962).
31. S. Chen, M.S. Thesis, Texas A&M University, Texas (1986).
32. R. Tamamushi, "Kinetic Parameters of Electrode Reactions of Metallic Compounds," p. 91, The Butterworth Group, London (1975).
33. C. R. Wilke and P. Chang, *AIChE J.*, **1,** 264 (1955).
34. A. J. Bard and L. R. Faulkner, "Electrochemical Methods: Fundamentals and Applications," p. 288, John Wiley & Sons, New York (1980).

Mass Transfer in Flow-Through Porous Electrodes with Two-Phase Liquid-Liquid Flow

James M. Fenton*,[1] and Richard C. Alkire*

Department of Chemical Engineering, University of Illinois, Urbana, Illinois 61801

ABSTRACT

The effect of two-phase liquid-liquid flow on mass transfer in flow-through porous electrodes where the current flow was perpendicular to the fluid flow was studied. Local reaction rates, concentrations, and potential distribution were measured along the direction of flow. Three systems were studied: (*i*) ferricyanide reduction in a solution containing no dispersed second phase; (*ii*) ferricyanide reduction in an aqueous solution containing toluene as an inert dispersed phase; and (*iii*) iodine reduction from an aqueous solution containing droplets of toluene in which the reactant was highly soluble in the organic phase. Experiments were carried out with controlled variation of solute concentration, dispersed phase void fraction and droplet size, and flow velocity. The overall mass-transfer rate was found to be a combination of four effects: (*i*) the single-phase mass-transfer rate associated with the liquid as if it were flowing alone through the porous electrode, (*ii*) the decrease in mass transfer owing to coverage of the electrode surface by dispersed liquid droplets, (*iii*) the mass-transfer exchange rate between the two liquids, and (*iv*) the further enhancement owing to penetration of the mass-transfer boundary layer by dispersed droplets containing the reactant. In general, it was found that the mass-transfer coefficient was not enhanced by addition of an inert second phase. However, when the dispersed phase contained dissolved reactant, the overall mass-transfer coefficient was increased substantially.

Since electrochemical reactions are heterogeneous in nature, high production rate industrial processes require a large electrode surface area and/or a high rate of transfer of reactant to and from the electrode.

To increase the mass-transfer rate one may increase either the driving force or the mass-transfer coefficient. To increase the driving force one could, for example, increase the solubility of the reacting species by adjustment of pH, by using a cosolvent, a second solvent miscible with water, or by using surfactant salts which solubilize micelles of reactant molecules. To increase the mass-transfer rate one could increase the surface area per unit reactor volume with porous electrodes, packed or trickle bed electrodes, or fluidized bed electrodes. In this study, the effect of introducing a second liquid phase for enhanc-

*Electrochemical Society Active Member.

[1]Present address: Department of Chemical Engineering, University of Connecticut, U-139, Storrs, Connecticut 06268.